



Published in final edited form as:

Neuroimage. 2009 May 1; 45(4): 1107–1116. doi:10.1016/j.neuroimage.2008.12.072.

CATEGORICAL AND CORRELATIONAL ANALYSES OF BASELINE FLUORODEOXYGLUCOSE POSITRON EMISSION TOMOGRAPHY IMAGES FROM THE ALZHEIMER'S DISEASE NEUROIMAGING INITIATIVE (ADNI)

Jessica B.S. Langbaum^{1,13}, Kewei Chen^{1,2,3,13}, Wendy Lee^{1,13}, Cole Reschke^{1,13}, Dan Bandy^{1,13}, Adam S. Fleisher^{1,12,13}, Gene E. Alexander^{4,13}, Norman L. Foster⁶, Michael W. Weiner^{7,8}, Robert A. Koeppe⁹, William J. Jagust¹⁰, Eric M. Reiman, M.D.^{1,5,11,13}, and the Alzheimer's Disease Neuroimaging Initiative

¹ Banner Alzheimer's Institute and Banner Good Samaritan PET Center, Phoenix, AZ

² Department of Mathematics, Arizona State University, Tempe, AZ

³ Department of Radiology, University of Arizona, Tucson, AZ

⁴ Department of Psychology and Evelyn F. McKnight Brain Institute, University of Arizona, Tucson, AZ

⁵ Department of Psychiatry, University of Arizona, Tucson, AZ

⁶ Center for Alzheimer's Care, Imaging and Research and Department of Neurology, University of Utah, Salt Lake City, UT

⁷ Center for Imaging of Neurodegenerative Diseases, San Francisco Veterans Affairs Medical Center

⁸ University of California at San Francisco, CA

⁹ Division of Nuclear Medicine, Department of Radiology, University of Michigan, Ann Arbor, MI

¹⁰ School of Public Health and Helen Wills Neuroscience Institute, University of California, Berkeley, CA

¹¹ Neurogenomics Division, Translational Genomics Research Institute, Phoenix, Arizona

¹² Department of Neurosciences, University of California, San Diego, San Diego, CA

¹³ Arizona Alzheimer's Consortium, Phoenix, AZ, USA

Abstract

Please address correspondence to Dr. Reiman at the Banner Alzheimer's Institute, 901 East Willetta Street, Phoenix, Arizona 85006; telephone: 602.239.6999; facsimile: 602.239.6253; eric.reiman@bannerhealth.com.

*Data used in the preparation of this article were obtained from the Alzheimer's Disease Neuroimaging Initiative (ADNI) database (www.loni.ucla.edu/ADNI). As such, the investigators within the ADNI contributed to the design and implementation of ADNI and/or provided data but did not participate in the analyses or writing of this report. ADNI investigators include (complete listing available at www.loni.ucla.edu/ADNI/Collaboration/ADNI_Manuscript_Citations.pdf).

Publisher's Disclaimer: This is a PDF file of an unedited manuscript that has been accepted for publication. As a service to our customers we are providing this early version of the manuscript. The manuscript will undergo copyediting, typesetting, and review of the resulting proof before it is published in its final citable form. Please note that during the production process errors may be discovered which could affect the content, and all legal disclaimers that apply to the journal pertain.

In mostly small single-center studies, Alzheimer's disease (AD) is associated with characteristic and progressive reductions in fluorodeoxyglucose positron emission tomography (PET) measurements of the regional cerebral metabolic rate for glucose (CMRgl). The AD Neuroimaging Initiative (ADNI) is acquiring FDG PET, volumetric magnetic resonance imaging, and other biomarker measurements in a large longitudinal multi-center study of initially mildly affected probable AD (pAD) patients, amnesic mild cognitive impairment (aMCI) patients, who are at increased AD risk, and cognitively normal controls (NC), and we are responsible for analyzing the PET images using statistical parametric mapping (SPM). Here we compare baseline CMRgl measurements from 74 pAD patients and 142 aMCI patients to those from 82 NC, we correlate CMRgl with categorical and continuous measures of clinical disease severity, and we compare apolipoprotein E (APOE) $\epsilon 4$ carriers to non-carriers in each of these subject groups. In comparison with NC, the pAD and aMCI groups each had significantly lower CMRgl bilaterally in posterior cingulate, precuneus, parietotemporal and frontal cortex. Similar reductions were observed when categories of disease severity or lower Mini-Mental State Exam (MMSE) scores were correlated with lower CMRgl. However, when analyses were restricted to the pAD patients, lower MMSE scores were significantly correlated with lower left frontal and temporal CMRgl. These findings from a large, multi-site study support previous single-site findings, supports the characteristic pattern of baseline CMRgl reductions in AD and aMCI patients, as well as preferential anterior CMRgl reductions after the onset of AD dementia.

Keywords

Alzheimer's disease; MCI; MMSE; Positron Emission Tomography

INTRODUCTION

Fluorodeoxyglucose positron emission tomography (FDG PET) studies reveal characteristic and progressive reductions in the cerebral metabolic rate for glucose (CMRgl) in patients with clinically characterized and subsequently autopsy confirmed Alzheimer's disease (AD) (Hoffman et al., 2000; Jagust et al., 2007; Mielke et al., 1996; Minoshima et al., 2001; Silverman et al., 2001) and in patients with mild cognitive impairment (MCI), who have an increased risk of AD neuropathology and subsequent conversion to probable AD (pAD, the term commonly used for the clinical diagnosis of Alzheimer's dementia) (Arnaiz et al., 2001; Drzezga et al., 2003; Drzezga et al., 2005; Minoshima et al., 1997). Similar CMRgl reductions have been reported in cognitively normal people with one or two copies of the apolipoprotein E (APOE) $\epsilon 4$ allele, a common AD susceptibility gene, many years before the anticipated onset of symptoms (Reiman et al., 1996; Reiman et al., 2001; Reiman et al., 2004; Reiman et al., 2005). These and other studies raise the possibility that FDG PET, along with other brain imaging and biomarker measurements, could be used for earlier detection and tracking of Alzheimer's disease, in the differential diagnosis of AD in patients with dementia and MCI, in the enrichment or stratification of research subjects in clinical trials of putative AD-slowing therapies, and in the rapid evaluation of putative AD-slowing, risk-reducing and prevention therapies.

In numerous single-center (Alexander et al., 2002; Chase et al., 1984; de Leon et al., 1983; Duara et al., 1986; Foster et al., 1983; Foster et al., 1984; Haxby et al., 1990; Hoffman et al., 2000; Ibanez et al., 1998; Jagust et al., 1988; McGeer et al., 1990; Minoshima et al., 1994; Minoshima et al., 1995; Smith et al., 1992). multi-center (Herholz et al., 2002; Mosconi et al., 2008b; Silverman et al., 2001) FDG PET studies, AD has been associated with significantly lower CMRgl bilaterally in the precuneus and posterior cingulate, parietal and temporal cortex, and also with lower CMRgl in the frontal cortex and whole brain in more severely affected patients. Lower CMRgl has been correlated with dementia severity, either by assessing the

correlation between performance on measures of overall cognitive function, such as the Mini-Mental State Exam [MMSE], and CMRgl reduction over all study participants, or by comparing subgroups based on measures of disease severity, such as the MMSE, Clinical Dementia Rating [CDR], or Global Deterioration Scale score (Chase et al., 1984; Choo et al., 2007; Foster et al., 1984; Minoshima et al., 1995; Mosconi, 2005; Silverman et al., 2001; Smith et al., 1992). The CMRgl reductions correspond to the spatial pattern of gray matter atrophy observed using volumetric magnetic resonance imaging (MRI) (Chételat et al., 2008) and they predict subsequent cognitive decline and the histopathological diagnosis of AD (Hoffman et al., 2000; Minoshima et al., 2001; Silverman et al., 2001). In longitudinal studies, the CMRgl reductions are progressive (Alexander et al., 2002; Haxby et al., 1990; Jagust et al., 1988; McGeer et al., 1990; Mosconi, 2005; Mosconi et al., 2007a; Smith et al., 1992), and offer greater statistical power than clinical endpoints in the evaluation of putative AD-slowing treatments (Alexander et al., 2002; Reiman and Langbaum, 2008).

In a smaller number of mostly small single-center FDG PET studies, amnesic mild cognitive impairment (aMCI) and non-amnesic MCI are associated with lower CMRgl in some of the same brain regions as pAD (de Leon et al., 2001; De et al., 2001; Drzezga et al., 2003; Mosconi et al., 2004; Mosconi, 2005; Mosconi et al., 2007b), including direct comparisons between MCI and pAD (De Santi et al., 2001; Mosconi et al., 2005; Mosconi et al., 2008b; Nestor et al., 2003), and in an automatically characterized hippocampal region-of-interest (Mosconi et al., 2005; Mosconi et al., 2008a). A similar pattern of hypometabolism in the posterior cingulate cortex and hippocampus was reported in a large, multi-center study which included 114 patients with MCI (Mosconi et al., 2008b). In related studies, lower CMRgl in some of these regions predicted subsequent rates of clinical conversion to probable AD (Arnaiz et al., 2001; Drzezga et al., 2003; Drzezga et al., 2005; Minoshima et al., 1997) are progressive and able to distinguish those who subsequently converted to pAD from those who remained stable during the same time-frames (Anchisi et al., 2005; de Leon et al., 2001; De Santi et al., 2001; Drzezga et al., 2003; Mosconi et al., 2004). In one very small study that needs to be replicated, lower CMRgl in a preselected posterior cingulate region of interest (ROI) and APOE ϵ 4 carrier or non-carrier status were used together to completely distinguish between aMCI patients who rapidly converted to pAD and those who remained stable during the same time frame (Drzezga et al., 2005).

The AD Neuroimaging Initiative (ADNI) was launched in 2003 by the National Institute on Aging (NIA), the National Institute of Biomedical Imaging and Bioengineering (NIBIB), the Food and Drug Administration (FDA), private pharmaceutical companies and non-profit organizations, as a \$60 million, 5-year public-private partnership. ADNI is a large, multi-center, longitudinal study of 822 older adults, including 188 initially mildly affected pAD patients, 405 aMCI patients, and 229 cognitively normal controls (NC) who are being followed at 58 clinical sites in the United States (Mueller et al., 2005). All of the subjects have clinical ratings, neuropsychological tests, 1.5T volumetric MRI, and blood and urine samples at every visit (most commonly every 6 months for 2–3 years depending on the subject group); half of the subjects also have FDG PET or 3T MRI at every visit; more recently, a smaller number of subjects have fibrillar amyloid imaging measurements using Pittsburgh Compound B (PIB) PET; and more than half of the subjects have agreed to baseline and one-year cerebrospinal fluid (CSF) measurements.

ADNI is intended to provide a public resource to the entire community, providing privacy-protected data and images, selected biological samples, and findings from a limited number of analyses. It is intended to assist in the early detection and tracking of AD, and to provide information that could be used to help in estimating sample sizes and designing clinical trials of putative AD-slowing treatments in pAD and aMCI patients using brain imaging and other biomarker endpoints, as well as lessen the time and cost of clinical trials. ADNI provides a

foundation to compare different brain imaging modalities and image-analysis techniques for each of these purposes. Along the way, it has begun to set standards for the selection of pAD and aMCI patients, the qualification of clinical and imaging sites in multi-center clinical trials, the acquisition and centralized pre-processing of MRI and PET images, use of MRI phantoms, and real-time quality-assurance and quality-control procedures in multi-center clinical trials. This study complements other multi-center FDG PET studies (Herholz et al., 2002; Mosconi et al., 2008b; Silverman et al., 2001), as well as other multi-center neuroimaging initiatives that have begun in other continents and countries following the ADNI example, including Europe, Japan, and Australia (Frisoni et al., 2008).

As members of the ADNI PET Coordinating Center, we are responsible for a small number of voxel-based FDG PET analyses using statistical parametric mapping (SPM). For this report, we provide a descriptive report of the comparisons between baseline CMRgl measurements from 74 pAD patients and 142 aMCI patients to those from 82 NC; we characterized correlations between three categorical measurements of clinical disease severity (i.e., NC, aMCI and pAD based on CDR scores), as well as correlations between a continuous measure of clinical disease severity (MMSE scores) and lower CMRgl using data from all 298 subjects; and we characterized correlations between the same continuous measure of clinical disease severity and lower CMRI within the pAD group. We predicted that pAD and aMCI patients would have significantly lower CMRgl than NC in precuneus and posterior cingulate, parietal, and temporal cortex; that the pAD group would also have lower CMRgl in frontal cortex; that clinical disease severity would be correlated with lower CMRgl in each of these regions when the analysis included all three subject groups, and that it would be correlated with lower CMRgl in frontal cortex when the analysis was restricted to those AD patients with dementia. Establishing that similar findings between previous single-site studies and large, multi-site studies can be obtained is critical as the field advances. Findings from the comparison of aMCI patients who subsequently converted to pAD and those who remain stable during the same time frame will be described in a separate report.

METHODS

Subjects

The primary goal of ADNI has been to test whether serial MRI, PET, other biological markers, and clinical and neuropsychological assessment can be combined to measure the progression of MCI and early AD. ADNI subjects were between the ages of 55–90 at the time of enrollment. Eligibility criteria for enrollment in one of the three specific groups are as follows. NC participants had an MMSE score of 24 or higher, a CDR score of 0, and no diagnosis of depression, aMCI, or dementia. aMCI participants had an MMSE score of 24 or higher, a subjective memory complaint, objective memory loss measured by education adjusted scores on the Wechsler Memory Scale Logical Memory II, a CDR of 0.5, absence of significant levels of impairment in other cognitive domains, preserved activities of daily living (ADLs), and an absence of dementia (Petersen et al., 2001). Mild AD participants were enrolled if they had an MMSE score between 20–26 (inclusive), a CDR score of 0.5 or 1.0, and met NINCDS/ADRDA criteria for probable AD (McKhann et al., 1984). For more information, please refer to the ADNI website (<http://www.adni-info.org/index.php>). Baseline FDG PET data from 298 ADNI participants (74 pAD, 142 aMCI, and 82 NC) acquired from Siemens, General Electric (GE), and Philips PET scanners were available for downloading from the ADNI Laboratory on NeuroImaging (LONI, University of California, Los Angeles) website (<http://www.loni.ucla.edu/ADNI/>). PET data acquired from the Siemens HRRT (n=51) and BioGraph HiRez (n=37) scanners were excluded from the primary analysis due to differences in the pattern of FDG uptake related to radiation attenuation, scatter and the subject's position in the scanner that were discovered during the data quality control and assurance checks.

However, as noted in the results section, we confirmed our main findings with only slightly smaller effect sizes when data from all of the scanners were included in a post-hoc analysis.

FDG PET

Data Acquisition

FDG PET scans were acquired according to a standardized protocol. Data presented in this paper were collected using 20 different PET scanners (7 GE models, 5 Philips models, and 8 Siemens models, not including the HRRT and BioGraph HiRez scanners). The proportion of subjects in each subject group did not differ significantly in the scanners used to acquire their FDG PET images ($\chi^2(51) = 21.9; p = 0.99$). A 30-min dynamic emission scan, consisting of 6 5-min frames, was acquired starting 30 min after the intravenous injection of 5.0 ± 0.5 mCi of ^{18}F -FDG, as the subjects, who were instructed to fast for at least four hours prior to the scan, lay quietly in a dimly lit room with their eyes open and minimal sensory stimulation. Data were corrected for radiation-attenuation and scatter using transmission scans from Ge-68 rotating rod sources and reconstructed using measured-attenuation correction and image reconstruction algorithms specified for each scanner (http://www.loni.ucla.edu/ADNI/Data/ADNI_Data.shtml). Following the scan, each image was reviewed for possible artifacts at the University of Michigan and all raw and processed study data was archived. The images were de-identified and transmitted to LONI for storage and pre-processing to correct for differences across PET scanners used at various ADNI sites.

Centralized FDG-PET Image Pre-Processing

The six five-min emission frames acquired in each subject 30–60 min following FDG administration were pre-processed at the University of Michigan according to the following steps to help correct for scanner-related differences in FDG uptake: First, each of the subject's emission frames were co-registered to his or her first frame and averaged. Second, each person's 30-min emission image was reoriented into an image consisting of $160 \times 160 \times 96$ 1.5 mm voxels, such that their horizontal sections were parallel to a section through the anterior and posterior commissures and normalized for the variation in absolute voxel intensity. At this step, none of the images were linearly or non-linearly deformed for individual differences in size and shape. Finally, a scanner-specific filter function, determined using scans acquired on the Hoffmann Brain phantom during the scanner certification process was used to ensure that all of the images had an isotropic spatial resolution of 8 mm full-width-at-half-maximum (FWHM). The specific filter functions were determined from the Hoffman phantom PET scans that were acquired during the certification process.

FDG-PET Image Analysis

Baseline FDG-PET images were downloaded from the ADNI LONI website in NIFTI format. Using SPM5 (<http://www.fil.ion.ucl.ac.uk/spm/>), each FDG-PET image was linearly and nonlinearly deformed to the Montreal Neurological Imaging (MNI) Template, smoothed to a spatial resolution of 12 mm full width-at-half maximum (FWHM) using a Gaussian Kernel, and normalized for the variation in whole brain measurements using proportionate scaling, and used to compute statistical parametric maps for each of the contrasts and correlations noted in the introduction. In the framework of ANOVA/General Linear Model (with pooled variance and degree of freedom), Student t-tests were used to compare FDG PET images from each of the patient groups to those from the NC on a voxel-by-voxel basis, generating statistical parametric maps of group-related reductions in regional-whole brain CMRgl ($p < 0.001$, uncorrected for multiple comparisons). In addition, linear regression was used to examine the association between disease severity, assessed either by disease category (CDR score of 0, 0.5, 1) or MMSE score and CMRgl reductions within the entire subject group and separately by MMSE score within the pAD group ($p < 0.001$, uncorrected for multiple comparisons). The

statistical maps from each analysis were superimposed onto a spatially standardized, volume-rendered MRI in the MNI coordinate space using a significance threshold of $p < 0.005$, uncorrected for multiple comparisons, for illustrative purposes. Significance levels were adjusted for false discovery rate (FDR-corrected), using the commonly accepted threshold of $p < 0.05$, for the group comparison analyses. This approach was selected rather than our usual practice of adjusting for the number of resolution elements in the AD-affected brain regions using small-volume correction procedure in SPM ($p < 0.05$) (Alexander et al., 2002) in order to make the results from the present study comparable to those from other studies, independent of each study's particular hypothesis. The results from the correlation analyses were not FDR-corrected given that the regions-of-interest can be regarded as pre-defined by the group comparison analyses. For the primary analyses, data from local maxima from the brain regions were extracted to compare mean differences in regional-to-whole brain across participant groups. Post-hoc analyses were conducted to examine the effects of age on the correlation between MMSE score and CMRgl reductions. Additionally, we examined CMRgl reduction in APOE $\epsilon 4$ carriers compared to non-carriers in each of the subject groups.

RESULTS

The subject groups' demographic characteristics, MMSE scores, and APOE $\epsilon 4$ gene doses are described in Table 1. The three groups did not differ significantly in their gender distribution. The pAD group was slightly older than the aMCI ($p < 0.01$) and had slightly fewer years of education compared to the NC group ($p < 0.04$). As expected, the pAD group had significantly lower MMSE scores than both the aMCI and NC groups ($p < 0.001$), and the aMCI group had significantly lower MMSE scores than the NC group ($p < 0.001$). Also as expected, the pAD and aMCI groups had a significantly higher proportion of subjects with one or two copies of the APOE $\epsilon 4$ allele ($p < 0.001$) than the NC group, and the three groups differed in the distribution of CDR scores ($p < 0.001$). Similarities between the proportions of aMCI and pAD patients with one or two copies of the APOE $\epsilon 4$ allele may support the use of ADNI's aMCI criteria for the identification of early AD. No significant differences were noted between the groups whether data from the HRRT and HiRez scanners were excluded or included in the analysis, although maximal significance levels were higher after excluding these potentially problematic scans.

In comparison with NC, the pAD and MCI groups each had significantly lower CMRgl in brain regions preferentially affected by AD, including the precuneus, posterior cingulate and parietotemporal regions, as well as the occipital cortex ($p < 0.001$ uncorrected for multiple comparisons) (Table 2; Figure 1). Additionally, compared to the NC group, both the pAD and aMCI groups had lower CMRgl bilaterally in the frontal cortex ($p < 0.001$, uncorrected), which has been suggested to be affected to a lesser degree than the posterior brain regions in previous PET studies. In comparison with each of the patient groups, the NC group exhibited increased CMRgl bilaterally in the cerebellum, occipital, and sensorimotor cortex ($p < 0.001$, uncorrected), reflecting relative sparing in these areas.

Examining the correlation between clinical disease severity and regional hypometabolism across all ADNI participants, we identified a significant relationship between higher CDR score (our categorical measure of disease severity) and lower CMRgl in brain regions preferentially affected by AD, including the posterior cingulate, precuneus, parietotemporal regions ($p < 0.001$ uncorrected) as well as the occipital cortex ($p < 0.001$ uncorrected) (Table 3; Figure 2A).

Using a different measure of disease severity across all ADNI participants, we identified a significant relationship between lower MMSE scores (our continuous measure of clinical disease severity) and lower CMRgl in the AD-related brain regions, including the, precuneus and parietotemporal regions ($p < 0.001$ uncorrected) as well as the occipital and frontal cortices

($p < 0.001$ uncorrected) (Table 4; Figures 2B and 3). A post-hoc analysis was conducted, adjusting for age given that the average age of the pAD participants was higher than that of the aMCI group. The results were nearly identical to the primary overall MMSE analysis, with the exception that the CMRgl reductions in the frontal cortex were observed bilaterally ($p < 0.001$, uncorrected).

Restricting the analysis to the pAD group, significant associations between lower MMSE scores and lower CMRgl were limited to the left frontal and temporal cortex, fusiform gyrus and striatum ($p < 0.001$, uncorrected) (Table 5; Figure 2C), suggesting that these anterior regions may be preferentially affected by AD after the onset of dementia. Though we observed asymmetry in the pAD group, a post-hoc hemisphere-wise comparison failed to find any asymmetric significance.

Within the NC group, the $\epsilon 4$ carriers had lower CMRgl than non-carriers in bilateral precuneus and left frontal cortex ($p < 0.001$, uncorrected), supporting previous findings that APOE $\epsilon 4$ carriers have abnormally low CMRgl in AD-affected brain regions before the onset of symptoms. Within the aMCI group, the $\epsilon 4$ carriers had lower CMRgl than non-carriers in an extensive region of the right temporal cortex ($p < 0.001$, uncorrected), another AD-affected region. Possible explanations for this finding include a higher proportion of AD cases in the MCI patients with this susceptibility gene, more advanced disease in the ApoE4 factors, or a combination of these and other factors. Within the pAD group, we found very few differences in the carriers compared to the non-carriers, with the carriers exhibiting minimal reductions bilaterally in the mid cingulate ($p < 0.001$, uncorrected).

While our primary analyses excluded data from the HRRT and HiRez scanners, all of our findings were confirmed with only slightly smaller effect sizes after including ADNI data from all of the scanners in our post-hoc analyses.

DISCUSSION

Findings from this large multi-center study confirm the previously characterized pattern of regional hypometabolism in pAD and aMCI found in single- and multi-center studies and implicate additional brain regions. Furthermore, they confirm the previously characterized correlation between severity of clinical impairment in a combined group of patients and controls, but suggest that the hypometabolism observed in the frontal brain regions is associated with a more severe disease state and may be indicative of potential disease progression. Lastly, the results provide additional support for the comparability of images obtained from multi-site studies using different PET scanners (Herholz et al., 1993; Herholz et al., 2002; Mosconi et al., 2008b; Silverman et al., 2001), at least with the scanner qualification, real-time quality-assurance and quality control procedures, and pre-processing standardization steps used in ADNI.

The findings from the present study indicate that compared to normal controls, both the pAD and aMCI participants exhibited similar patterns of reduced CMRgl in posterior cingulate, precuneus, parietotemporal, frontal and occipital regions. Although the patterns of reductions were comparable, the magnitude and spatial extent of hypometabolism was greater among the pAD participants, and these patient group differences were not solely attributable to the effects of slightly older age in the AD group. These results, along with the relatively higher percentage of APOE $\epsilon 4$ carriers, add to the evidence that a significant proportion of patients meeting the aMCI criteria used in this study have early AD. Our ongoing longitudinal assessments will permit us to further characterize rates of clinical conversion to pAD, and determine the extent to which regional CMRgl reductions, alone or in combination with other measurements and risk factors, predicts clinical conversion to pAD.

Previous studies have reported significant correlations between clinical disease severity and lower MMSE scores and lower CMRgl in patients with pAD in posterior cingulate, precuneus, parietotemporal and frontal cortex (Bokde et al., 2005; Chase et al., 1984; Foster et al., 1983; Kawano et al., 2001; Mielke et al., 1992; Minoshima et al., 1995). Generally speaking, the results from the present study are in agreement with findings from previous studies and are noteworthy given the number of participants and the selection of pAD patients based on relatively mild clinical severity. In addition, we found a relationship between hypometabolism in the occipital cortex and greater disease severity, which, has been reported in some but not all FDG PET studies of AD (e.g., Alexander et al., 2002), but which has also been suggested to distinguish dementia with Lewy bodies (DLB) from AD (Minoshima et al., 2001). This finding might be partly attributable to our relatively large samples, permitting us to detect more subtle group differences than in some of the smaller single-center studies, and it may be partly related to the finding of preferential fibrillar amyloid-beta burden in AD patients (Klunk et al., 2004), which has been suggested to reflect cerebral amyloid angiopathy (Greenberg et al., 2008; Johnson et al., 2007). It also is possible that some of these individuals may have unsuspected Lewy body pathology, although the presence of Parkinsonian signs was exclusionary at enrollment.

When the analysis was restricted to only participants with pAD, the significant correlations between lower MMSE scores and lower CMRgl were limited to left frontal and temporal brain regions, suggesting that these regions may be preferentially affected after the onset of dementia. Hypometabolism in the left frontal and temporal brains regions has previously been reported in a longitudinal PET study of AD and may be considered to be relevant to progressive decline after the onset of dementia (Alexander et al., 2002; Choo et al., 2007). While we did observe lateralized CMRgl reductions, the post-hoc hemisphere-wise comparisons did not find any asymmetric significance. Preliminary findings (unpublished) from the longitudinal ADNI data suggest that, for mild pAD individuals, the posterior regions may still exhibit CMRgl decline initially, but, over a larger range of clinical decline and longer duration, we postulate that the declines in the posterior regions may abate with stronger frontal declines.

We did not find significant correlations between lower MMSE scores and lower CMRgl in the aMCI or NC groups. The absence of significant associations could be attributable to the modest range of MMSE scores in these groups, heterogeneity in the aMCI group, or a combination of these and other factors. It is possible that other neuropsychological measurements or clinical ratings could provide a more sensitive measure of cognitive decline and these subject groups, and that these measures be associated with lower CMRgl in brain regions preferentially affected by AD or normal aging. For instance, in a study with aMCI patients using annual change on the Mattis dementia rating scale as the measure of disease severity, the authors identified a significant positive relationship between CMRgl and disease severity in the right lateral temporo-parietal and bilateral medial frontal regions (Chételat et al., 2005). Examining the association between CDR sum of boxes (CDR-SB) and CMRgl in patients with aMCI, another team reported a voxel-based inverse association in the right posterior cingulate gyrus, although it did not survive correction for multiple comparisons (Pernecky et al., 2007).

Analyzing the effects of the APOE $\epsilon 4$ allele, cognitively normal $\epsilon 4$ carriers had lower CMRgl than non-carriers in several AD-affected precuneus and frontal regions, confirming findings from previous single-center studies (Reiman et al., 1996; Reiman et al., 2004; Reiman et al., 2005; Small et al., 1995). Still, these findings were less extensive than those reported in our own studies of cognitively normal late-middle-aged carriers and non-carriers, perhaps reflecting the combined effects of slightly older age and differential survivor bias, the inclusion of subjects who were less closely matched for age, gender and educational level, reduced sensitivity due to the inclusion of data from multiple scanners, or other factors. In aMCI patients, normal $\epsilon 4$ carriers had lower CMRgl than non-carriers in AD-affected lateral temporal

regions, which could reflect a higher proportion of AD cases in the MCI patients with this susceptibility gene, more advanced disease in the APOE ϵ 4 carriers, or a combination of these and other factors. Additional analyses are needed to further clarify the extent to which APOE ϵ 4 gene dose, the pattern of cerebral hypometabolism, or a combination of these and other factors predict subsequent rates of conversion to probable AD. Within the pAD group, we found very few differences in the carriers compared to the non-carriers, suggesting that the pattern of FDG hypometabolism in probable AD patients is not attributable to effects of the APOE ϵ 4 allele independent of AD itself.

Among its important goals, ADNI is intended to help in the design and performance of multi-center clinical trials of putative AD-slowing treatments. ADNI has already developed and successfully implemented the protocols used to acquire 1.5T MRI, 3T MRI, FDG PET and PIB PET images in a standardized way, helping to account for differences among imaging systems, and demonstrating comparability in the quality of images on most--but not all--of the imaging systems assessed. Second, it has already developed and successfully implemented the site-qualification, real-time quality-assurance, image-preprocessing, and centralized data management procedures needed to provide high-quality data. Third, it has demonstrated the feasibility of collecting CSF samples in a high proportion of study participants. Fourth, it has already begun to provide data and specimens for the early detection and tracking of AD. Fifth, ADNI provides the means to evaluate promising new image analysis techniques and biomarker measurements, comparing them to existing methods and measurements in the early detection and tracking of AD. Perhaps most important, ADNI researchers have begun to characterize and directly compare different imaging methods, data analysis methods, and biomarkers in their ability to distinguish subject groups, their ability to predict rates of cognitive decline and clinical progression from MCI to probable AD, and their statistical power to evaluate putative β -amyloid-modifying and disease-slowing treatments in multi-center clinical trials, thereby facilitating the potential use of these methods for participant stratification or enrichment in clinical trials.

This study has several limitations. As previously mentioned, the MMSE is only one potential measure of disease severity and overall cognitive functioning. In addition, the ADNI study is not an epidemiological sample and may not be representative for all cognitively healthy older adults, aMCI, or mild pAD patients. Participants in ADNI were recruited primarily from subspecialty memory clinics and Alzheimer's research centers, have unusually high levels of education, and included more males than females, and may have other factors that reflect their level of motivation required to participate in this demanding study. The study was not designed to test the diagnostic utility of imaging. Participants were highly selected and patients with concurrent medical, neurological, and psychiatric illness, or atypical features were excluded. Thus the study population does not reflect the diversity of patient characteristics seen in clinical practice. Furthermore, our MCI findings are restricted to the amnesic MCI subtype and may not be applicable to MCI patients with different cognitive profiles. Lastly, while every attempt was made to ensure that participants assigned to each subgroup were in fact cognitively healthy, had aMCI or pAD, there is always the possibility that some participants were misclassified when it comes to their underlying neuropathology. In our initial assessment of image quality, we found potentially confounding patterns of FDG uptake in the reconstructed images acquired on Siemens HRRT and BioGraph HiRez scanners, causing us to eliminate these scans from our primary analysis, though the findings were similar when these scans were included in our post-hoc analyses. (It remains to be determined what effect the inclusion of these or other scanners might have in terms of the power to detect or track AD-related changes in multi-center trials. .). Further, it remains possible that additional refinements in image reconstruction may reduce the variability initially associated with these scanners.

In conclusion, findings from this and other single-site and multi-center studies support the characteristic pattern of preferential posterior cingulate, precuneus, parietotemporal CMRgl reductions previously found in AD and aMCI patients, as well as preferential anterior CMRgl reductions after the onset of dementia.

Acknowledgments

The authors thank Patti Aguilar, Napatkamon Ayutyanont, David Branch, Sandra Goodwin, Debbie Intorcía, Jennifer Keppler, Xiofen Liu, Les Mullen, Anita Prouty, Stephanie Reeder, Sydney Schilcher, Desiree Van Egmond, and Justin Venditti for their technical assistance.

Data collection and sharing for this project was funded by the Alzheimer's Disease Neuroimaging Initiative (ADNI; Principal Investigator: Michael Weiner; NIH grant U01 AG024904). ADNI is funded by the National Institute on Aging, the National Institute of Biomedical Imaging and Bioengineering (NIBIB), and through generous contributions from the following: Pfizer Inc., Wyeth Research, Bristol-Myers Squibb, Eli Lilly and Company, GlaxoSmithKline, Merck & Co. Inc., AstraZeneca AB, Novartis Pharmaceuticals Corporation, Alzheimer's Association, Eisai Global Clinical Development, Elan Corporation plc, Forest Laboratories, and the Institute for the Study of Aging, with participation from the U.S. Food and Drug Administration. Industry partnerships are coordinated through the Foundation for the National Institutes of Health. The grantee organization is the Northern California Institute for Research and Education, and the study is coordinated by the Alzheimer's Disease Cooperative Study at the University of California, San Diego. ADNI data are disseminated by the Laboratory of Neuro Imaging at the University of California, Los Angeles.

Reference List

- Alexander GE, Chen K, Pietrini P, Rapoport SI, Reiman EM. Longitudinal PET evaluation of cerebral metabolic decline in dementia: A potential outcome measure in Alzheimer's disease treatment studies. *Am J Psychiatry* 2002;159:738–745. [PubMed: 11986126]
- Anchisi D, Borroni B, Franceschi M, Kerrouche N, Kalbe E, Beuthien-Beumann B, Cappa S, Lenz O, Ludecke S, Marcone A, Mielke R, Ortelli P, Padovani A, Pelati O, Pupi A, Scarpini E, Weisenbach S, Herholz K, Salmon E, Holthoff V, Sorbi S, Fazio F, Perani D. Heterogeneity of brain glucose metabolism in mild cognitive impairment and clinical progression to Alzheimer disease. *Arch Neurol* 2005;62:1728–1733. [PubMed: 16286547]
- Arnaiz E, Jelic V, Almkvist O, Wahlund LO, Winblad B, Valind S, Nordberg A. Impaired cerebral glucose metabolism and cognitive functioning predict deterioration in mild cognitive impairment. *Neuroreport* 2001;12:851–855. [PubMed: 11277595]
- Bokde AL, Teipel SJ, Drzezga A, Thissen J, Bartenstein P, Dong W, Leinsinger G, Born C, Schwaiger M, Moeller HJ, Hampel H. Association between cognitive performance and cortical glucose metabolism in patients with mild Alzheimer's disease. *Dement Geriatr Cogn Disord* 2005;20:352–357. [PubMed: 16192725]
- Chase TN, Foster NL, Fedio P, Brooks R, Mansi L, Di Chiro G. Regional cortical dysfunction in Alzheimer's disease as determined by positron emission tomography. *Ann Neurol* 1984;15 (Suppl):S170–S174. [PubMed: 6611118]
- Chételat G, Desgranges B, Landeau B, Mézence F, Poline JB, de la Sayette V, Viader F, Eustache F, Baron JC. Direct voxel-based comparison between grey matter hypometabolism and atrophy in Alzheimer's disease. *Brain* 2008;131:60–71. [PubMed: 18063588]
- Chételat G, Eustache F, Viader F, de la Sayette V, Pélerin A, Mézence F, Hannequin D, Dupuy B, Baron JC, Desgranges B. FDG-PET measurement is more accurate than neuropsychological assessments to predict global cognitive deterioration in patients with mild cognitive impairment. *Neurocase* 2005;11:14–25. [PubMed: 15804920]
- Choo IH, Lee DY, Youn JC, Jhoo JH, Kim KW, Lee DS, Lee JS, Woo JI. Topographic patterns of brain functional impairment progression according to clinical severity staging in 116 Alzheimer disease patients: FDG-PET study. *Alzheimer Dis Assoc Disord* 2007;21:77–84. [PubMed: 17545731]
- de Leon MJ, Convit A, Wolf OT, Tarshish CY, DeSanti S, Rusinek H, Tsui W, Kandil E, Scherer AJ, Roche A, Imossi A, Thorn E, Bobinski M, Caraos C, Lesbre P, Schlyer D, Poirier J, Reisberg B, Fowler J. Prediction of cognitive decline in normal elderly subjects with 2-[(18)F]fluoro-2-deoxy-D-glucose/

- positron-emission tomography (FDG/PET). *Proc Natl Acad Sci USA* 2001;98:10966–10971. [PubMed: 11526211]
- de Leon MJ, Ferris SH, George AE, Reisberg B, Christman DR, Kricheff II, Wolf AP. Computed tomography and positron emission transaxial tomography evaluations of normal aging and Alzheimer's disease. *J Cereb Blood Flow Metab* 1983;3:391–394. [PubMed: 6603463]
- De Santi S, de Leon MJ, Rusinek H, Convit A, Tarshish CY, Roche A, Tsui WH, Kandil E, Boppana M, Daisley K, Wang GJ, Schlyer D, Fowler J. Hippocampal formation glucose metabolism and volume losses in MCI and AD. *Neurobiol Aging* 2001;22:529–539. [PubMed: 11445252]
- De SS, de Leon MJ, Rusinek H, Convit A, Tarshish CY, Roche A, Tsui WH, Kandil E, Boppana M, Daisley K, Wang GJ, Schlyer D, Fowler J. Hippocampal formation glucose metabolism and volume losses in MCI and AD. *Neurobiol Aging* 2001;22:529–539. [PubMed: 11445252]
- Drzezga A, Grimmer T, Riemenschneider M, Lautenschlager N, Siebner H, Alexopoulos P, Minoshima S, Schwaiger M, Kurz A. Prediction of individual clinical outcome in MCI by means of genetic assessment and (18)F-FDG PET. *J Nucl Med* 2005;46:1625–1632. [PubMed: 16204712]
- Drzezga A, Lautenschlager N, Siebner H, Riemenschneider M, Willoch F, Minoshima S, Schwaiger M, Kurz A. Cerebral metabolic changes accompanying conversion of mild cognitive impairment into Alzheimer's disease: a PET follow-up study. *Eur J Nucl Med Mol Imaging* 2003;30:1104–1113. [PubMed: 12764551]
- Duara R, Grady CL, Haxby JV. Positron emission tomography in Alzheimer's disease. *Neurology* 1986;879–887. [PubMed: 3487046]
- Foster NL, Chase TN, Fedio P, Patronas NJ, Brooks RA, Di Chiro G. Alzheimer's disease: focal cortical changes shown by positron emission tomography. *Neurology* 1983;33:961–965. [PubMed: 6603596]
- Foster NL, Chase TN, Mansi L, Brooks R, Fedio P, Patronas NJ, Di Chiro G. Cortical abnormalities in Alzheimer's disease. *Ann Neurol* 1984;16:649–654. [PubMed: 6335378]
- Frisoni GB, Henneman WJP, Weiner MW, Scheltens P, Vellas B, Reynish E, Hudecova J, Hampel H, Burger K, Blennow K, Waldemar G, Johannsen P, Wahlund LO, Zito G, Rossini PM, Winblad B, Barkhof F. The pilot European Alzheimer's Disease Neuroimaging Initiative of the European Alzheimer's Disease Consortium. *Alzheimer's & Dementia* 2008;4:255–264.
- Greenberg SM, Grabowski T, Gurol ME, Skehan ME, Nandigam RN, Becker JA, Garcia-Alloza M, Prada C, Frosch MP, Rosand J, Viswanathan A, Smith EE, Johnson KA. Detection of isolated cerebrovascular beta-amyloid with Pittsburgh compound B. *Ann Neurol* 2008;64:587–591. [PubMed: 19067370]
- Haxby JV, Grady CL, Koss E, Horwitz B, Heston L, Schapiro M, Friedland RP, Rapoport SI. Longitudinal study of cerebral metabolic asymmetries and associated neuropsychological patterns in early dementia of the Alzheimer type. *Arch Neurol* 1990;47:753–760. [PubMed: 2357155]
- Herholz K, Perani D, Salmon E, Franck G, Fazio F, Heiss WD, Comar D. Comparability of FDG PET studies in probable Alzheimer's disease. *The Journal of Nuclear Medicine* 1993;34:1460–1466.
- Herholz K, Salmon E, Perani D, Baron JC, Holthoff V, Frolich L, Schonknecht P, Ito K, Mielke R, Kalbe E, Zundorf G, Delbeuck X, Pelati O, Anchisi D, Fazio F, Kerrouche N, Desgranges B, Eustache F, Beuthien-Baumann B, Menzel C, Schroder J, Kato T, Arahata Y, Henze M, Heiss WD. Discrimination between Alzheimer dementia and controls by automated analysis of multicenter FDG PET. *Neuroimage* 2002;17:302–316. [PubMed: 12482085]
- Hoffman JM, Welsh-Bohmer KA, Hanson M, Crain B, Hulette C, Earl N, Coleman RE. FDG PET imaging in patients with pathologically verified dementia. *J Nucl Med* 2000;41:1920–1928. [PubMed: 11079505]
- Ibanez V, Pietrini P, Alexander GE, Furey ML, Teichberg D, Rajapakse JC, Rapoport SI, Schapiro MB, Horwitz B. Regional glucose metabolic abnormalities are not the result of atrophy in Alzheimer's disease. *Neurology* 1998;50:1585–1593. [PubMed: 9633698]
- Jagust W, Reed B, Mungas D, Ellis W, DeCarli C. What does fluorodeoxyglucose PET imaging add to a clinical diagnosis of dementia? *Neurology* 2007;69:871–877. [PubMed: 17724289]
- Jagust WJ, Friedland RP, Budinger TF, Koss E, Ober B. Longitudinal studies of regional cerebral metabolism in Alzheimer's disease. *Neurology* 1988;38:909–912. [PubMed: 3259296]
- Johnson KA, Gregas M, Becker JA, Kinnecom C, Salat DH, Moran EK, Smith EE, Rosand J, Rentz DM, Klunk WE, Mathis CA, Price JC, DeKosky ST, Fischman AJ, Greenberg SM. Imaging of amyloid

burden and distribution in cerebral amyloid angiopathy. *Ann Neurol* 2007;62:229–234. [PubMed: 17683091]

Kawano M, Ichimiya A, Ogomori K, Kuwabara Y, Sasaki M, Yoshida T, Tashiro N. Relationship between both IQ and Mini-Mental State Examination and the regional cerebral glucose metabolism in clinically diagnosed Alzheimer's disease: a PET study. *Dement Geriatr Cogn Disord* 2001;12:171–176. [PubMed: 11173892]

Klunk WE, Engler H, Nordberg A, Wang Y, Blomqvist G, Holt DP, Bergstrom M, Savitcheva I, Huang GF, Estrada S, Ausen B, Debnath ML, Barletta J, Price JC, Sandell J, Lopresti BJ, Wall A, Koivisto P, Antoni G, Mathis CA, Langstrom B. Imaging brain amyloid in Alzheimer's disease with Pittsburgh Compound-B. *Ann Neurol* 2004;55:306–319. [PubMed: 14991808]

McGeer EG, Peppard RP, McGeer PL, Tuokko H, Crockett D, Parks R, Akiyama H, Calne DB, Beattie BL, Harrop R. 18Fluorodeoxyglucose positron emission tomography studies in presumed Alzheimer cases, including 13 serial scans. *Can J Neurol Sci* 1990;17:1–11. [PubMed: 2311010]

McKhann G, Drachman D, Folstein M, Katzman R, Price D, Stadlan EM. Clinical diagnosis of Alzheimer's disease: report of the NINCDS-ADRDA Work Group under the auspices of Department of Health and Human Services Task Force on Alzheimer's Disease. *Neurology* 1984;34:939–944. [PubMed: 6610841]

Mielke R, Herholz K, Grond M, Kessler J, Heiss WD. Differences of regional cerebral glucose metabolism between presenile and senile dementia of Alzheimer type. *Neurobiol Aging* 1992;13:93–98. [PubMed: 1542386]

Mielke R, Schroder R, Fink GR, Kessler J, Herholz K, Heiss WD. Regional cerebral glucose metabolism and postmortem pathology in Alzheimer's disease. *Acta Neuropathol* 1996;91:174–179. [PubMed: 8787151]

Minoshima S, Foster NL, Kuhl DE. Posterior cingulate cortex in Alzheimer's disease. *Lancet* 1994;344:895. [PubMed: 7916431]

Minoshima S, Foster NL, Sima AA, Frey KA, Albin RL, Kuhl DE. Alzheimer's disease versus dementia with Lewy bodies: cerebral metabolic distinction with autopsy confirmation. *Ann Neurol* 2001;50:358–365. [PubMed: 11558792]

Minoshima S, Frey KA, Koeppe RA, Foster NL, Kuhl DE. A diagnostic approach in Alzheimer's disease using three-dimensional stereotactic surface projections of fluorine-18-FDG PET. *J Nucl Med* 1995;36:1238–1248. [PubMed: 7790950]

Minoshima S, Giordani B, Berent S, Frey KA, Foster NL, Kuhl DE. Metabolic reduction in the posterior cingulate cortex in very early Alzheimer's disease. *Ann Neurol* 1997;42:85–94. [PubMed: 9225689]

Mosconi L. Brain glucose metabolism in the early and specific diagnosis of Alzheimer's disease. FDG-PET studies in MCI and AD. *Eur J Nucl Med Mol Imaging* 2005;32:486–510. [PubMed: 15747152]

Mosconi L, De SS, Li J, Tsui WH, Li Y, Boppana M, Laska E, Rusinek H, de Leon MJ. Hippocampal hypometabolism predicts cognitive decline from normal aging. *Neurobiol Aging*. 2007a

Mosconi L, De SS, Li J, Tsui WH, Li Y, Boppana M, Laska E, Rusinek H, de Leon MJ. Hippocampal hypometabolism predicts cognitive decline from normal aging. *Neurobiol Aging* 2008a;29:676–692. [PubMed: 17222480]

Mosconi L, Perani D, Sorbi S, Herholz K, Nacmias B, Holthoff V, Salmon E, Baron JC, De Cristofaro MT, Padovani A, Borroni B, Franceschi M, Bracco L, Pupi A. MCI conversion to dementia and the APOE genotype: a prediction study with FDG-PET. *Neurology* 2004;63:2332–2340. [PubMed: 15623696]

Mosconi L, Tsui WH, De SS, Li J, Rusinek H, Convit A, Li Y, Boppana M, de Leon MJ. Reduced hippocampal metabolism in MCI and AD: automated FDG-PET image analysis. *Neurology* 2005;64:1860–1867. [PubMed: 15955934]

Mosconi L, Tsui WH, Herholz K, Pupi A, Drzezga A, Lucignani G, Reiman EM, Holthoff V, Kalbe E, Sorbi S, ehl-Schmid J, Perneczky R, Clerici F, Caselli R, Beuthien-Baumann B, Kurz A, Minoshima S, de Leon MJ. Multicenter standardized 18F-FDG PET diagnosis of mild cognitive impairment, Alzheimer's disease, and other dementias. *The Journal of Nuclear Medicine* 2008b;49:390–398.

Mosconi L, Tsui WH, Pupi A, De SS, Drzezga A, Minoshima S, de Leon MJ. (18)F-FDG PET database of longitudinally confirmed healthy elderly individuals improves detection of mild cognitive impairment and Alzheimer's disease. *J Nucl Med* 2007b;48:1129–1134. [PubMed: 17574982]

- Mueller SG, Weiner MW, Thal LJ, Petersen RC, Jack CR, Jagust W, Trojanowski JQ, Toga AW, Beckett L. Ways toward an early diagnosis in Alzheimer's disease: The Alzheimer's Disease Neuroimaging Initiative (ADNI). *Alzheimers Dement* 2005;1:55–66. [PubMed: 17476317]
- Nestor PJ, Fryer TD, Smielewski P, Hodges JR. Limbic hypometabolism in Alzheimer's disease and mild cognitive impairment. *Ann Neurol* 2003;54:343–351. [PubMed: 12953266]
- Perneczky R, Hartmann J, Grimmer T, Drzezga A, Kurz A. Cerebral metabolic correlates of the clinical dementia rating scale in mild cognitive impairment. *J Geriatr Psychiatry Neurol* 2007;20:84–88. [PubMed: 17548777]
- Petersen RC, Doody R, Kurz A, Mohs RC, Morris JC, Rabins PV, Ritchie K, Rossor M, Thal L, Winblad B. Current concepts in mild cognitive impairment. *Arch Neurol* 2001;58:1985–1992. [PubMed: 11735772]
- Reiman EM, Langbaum, JBS. Brain imaging in the evaluation of putative Alzheimer's disease slowing, risk-reducing and prevention therapies. In: Jagust, WJ.; D'Esposito, M., editors. *Imaging and the Aging Brain*. Oxford University Press; New York: 2008.
- Reiman EM, Caselli RJ, Chen K, Alexander GE, Bandy D, Frost J. Declining brain activity in cognitively normal apolipoprotein E ϵ 4 heterozygotes: A foundation for using positron emission tomography to efficiently test treatments to prevent Alzheimer's disease. *Proc Natl Acad Sci USA* 2001;98:3334–3339. [PubMed: 11248079]
- Reiman EM, Caselli RJ, Yun LS, Chen K, Bandy D, Minoshima S, Thibodeau SN, Osborne D. Preclinical evidence of Alzheimer's disease in persons homozygous for the ϵ 4 allele for apolipoprotein E. *N Engl J Med* 1996;334:752–758. [PubMed: 8592548]
- Reiman EM, Chen K, Alexander GE, Caselli RJ, Bandy D, Osborne D, Saunders AM, Hardy J. Functional brain abnormalities in young adults at genetic risk for late-onset Alzheimer's dementia. *Proc Natl Acad Sci USA* 2004;101:284–289. [PubMed: 14688411]
- Reiman EM, Chen K, Alexander GE, Caselli RJ, Bandy D, Osborne D, Saunders AM, Hardy J. Correlations between apolipoprotein E ϵ 4 gene dose and brain-imaging measurements of regional hypometabolism. *Proc Natl Acad Sci USA* 2005;102:8299–8302. [PubMed: 15932949]
- Silverman DH, Small GW, Chang CY, Lu CS, Kung De Aburto MA, Chen W, Czernin J, Rapoport SI, Pietrini P, Alexander GE, Schapiro MB, Jagust WJ, Hoffman JM, Welsh-Bohmer KA, Alavi A, Clark CM, Salmon E, de Leon MJ, Mielke R, Cummings JL, Kowell AP, Gambhir SS, Hoh CK, Phelps ME. Positron emission tomography in evaluation of dementia: Regional brain metabolism and long-term outcome. *JAMA* 2001;286:2120–2127. [PubMed: 11694153]
- Small GW, Mazziotta JC, Collins MT, Baxter LR, Phelps ME, Mandelkern MA, Kaplan A, La Rue A, Adamson CF, Chang L. Apolipoprotein E type 4 allele and cerebral glucose metabolism in relatives at risk for familial Alzheimer disease. *JAMA* 1995;273:942–947. [PubMed: 7884953]
- Smith GS, de Leon MJ, George AE, Kluger A, Volkow ND, McRae T, Golomb J, Ferris SH, Reisberg B, Ciaravino J. Topography of cross-sectional and longitudinal glucose metabolic deficits in Alzheimer's disease. Pathophysiologic implications. *Arch Neurol* 1992;49:1142–1150. [PubMed: 1444881]
- Talairach, J.; Tournoux, P. *Co-Planar Stereotaxic Atlas of the Human Brain*. Thieme Medical Publishers; New York: 1988.

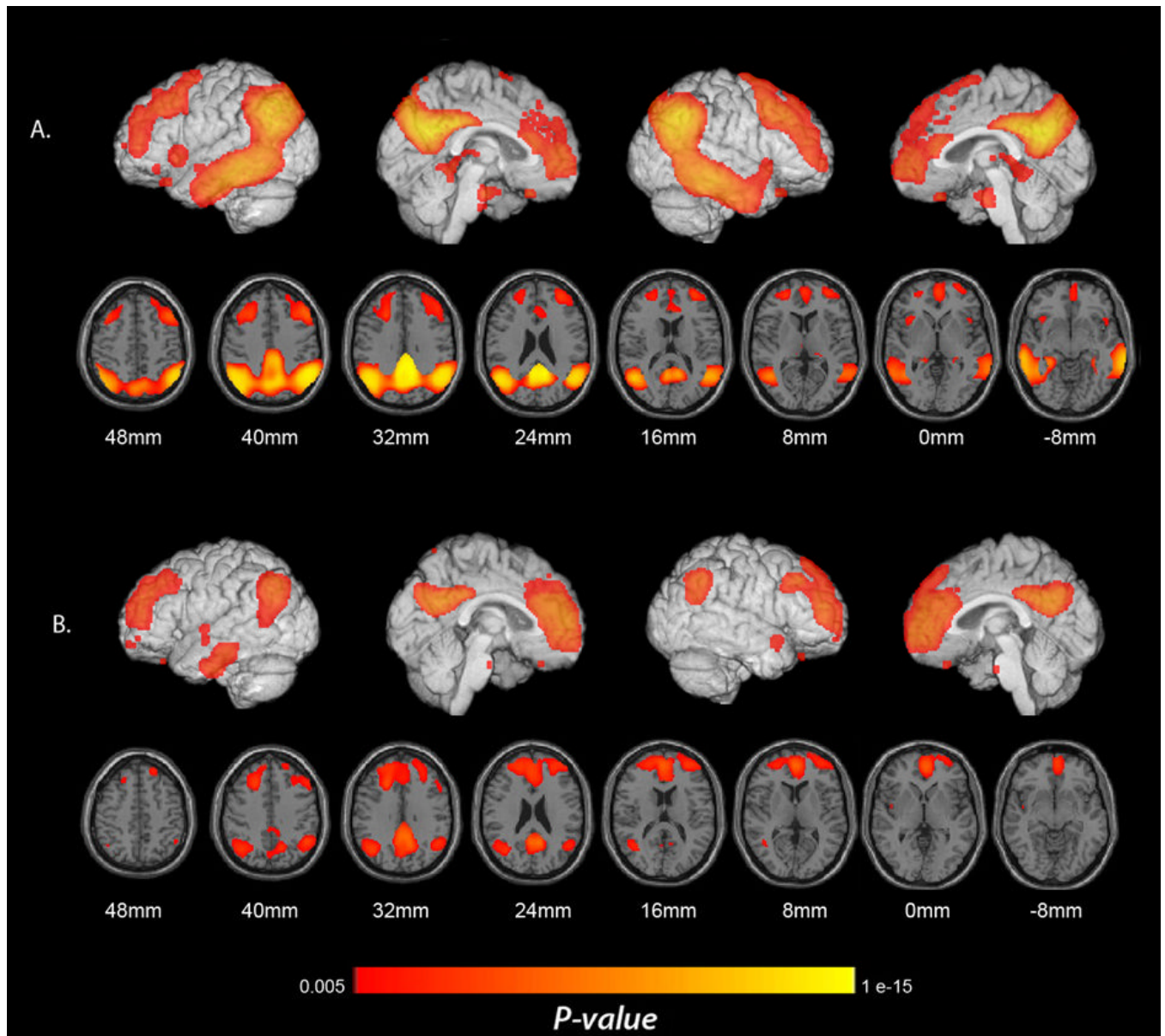


Figure 1. Regions with significantly lower CMRgl in pAD and aMCI patients. (A) Lower CMRgl in pAD patients than in elderly NC. (B) Lower CMRgl in aMCI patients than in elderly NC ($p < 0.005$, uncorrected for multiple comparisons). Significance levels in these brain maps are uncorrected for multiple comparisons. Findings are projected on to the lateral and medial surfaces of the left and right cerebral hemispheres and are also shown on horizontal sections in relationship to a horizontal section between the anterior and posterior commissures.

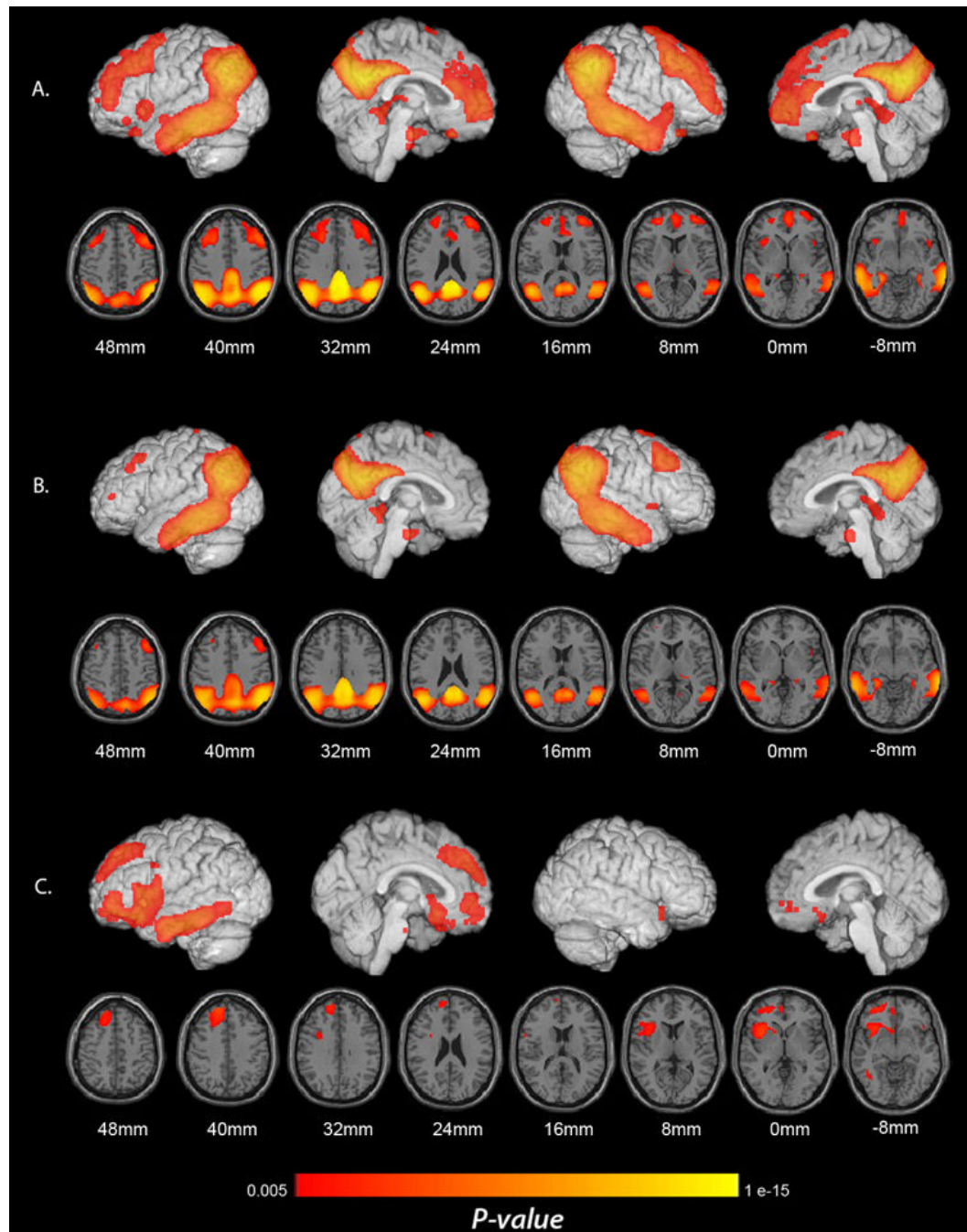


Figure 2.

Significant correlations between clinical disease severity and lower CMRgl. (A) Correlations between higher CDR score (a categorical measure of clinical disease severity) and lower CMRgl using data from the three subject groups. (B) Correlations between lower MMSE score (a continuous measure of clinical disease severity) and lower CMRgl using data from the three subject groups. (C). Correlations between lower MMSE score and lower CMRgl when the analysis is restricted to the pAD group. Significance levels in these brain maps are uncorrected for multiple comparisons. Findings are projected on to the lateral and medial surfaces of the left and right cerebral hemispheres and are also shown on horizontal sections in relationship to a horizontal section between the anterior and posterior commissures.

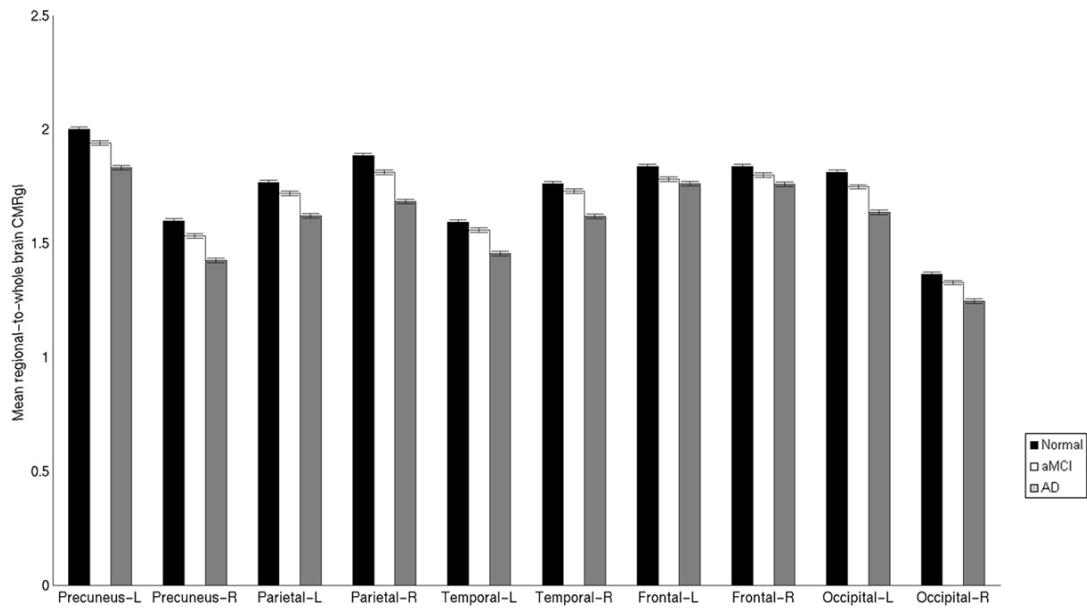


Figure 3. Mean regional-to-whole brain CMRgl in ten different brain regions between Normal, aMCI, and pAD groups. Error bars represent the standard error of the mean. For each region displayed in Table 4, data from the local maxima was extracted and used to compare the mean regional-to-whole brain CMRgl between patient groups

TABLE 1

Probable AD, Amnesic MCI and Normal Control Group Characteristics

	NC (n = 82)	aMCI (n = 142)	pAD (n = 74)	P-VALUE
Age (mean ± SD)	68.4±10.3	66.3±11.9	71.1±10.1	0.01 ^a
Gender (% Male/Female)	22/78	20/80	34/66	0.08
MMSE Score (mean ± SD)	29.0±1.1	27.1±1.7	23.2±2.2	< 0.001 ^{a,b,c}
CDR Severity Score (%)				
0	100	0.7	0	
0.5	0	99.3	37.8	< 0.001 ^{a,b,c}
1.0	0	0	62.2	
APOE ε4 Gene Dose (%)				
No copies	74.4	45.1	35.1	
One copy	23.2	40.8	47.3	< 0.001 ^{b,c}
Two copies	2.4	14.1	17.6	
Years of education (mean ± SD)	15.9±2.8	15.3±2.7	14.8±3.3	0.04 ^b

Baseline demographic differences between NC, aMCI, and AD participants were analyzed using one-way analysis of variance (ANOVA), Fisher's exact and Chi-square (χ^2) tests. Scheffé-multiple comparison test was used to compare the differences between each pair of means.

^a pAD significantly different from aMCI

^b pAD significantly different from NC

^c aMCI significantly different from NC

TABLE 2

Location and magnitude of the most significant between-group differences in regional-to-whole brain CMRgl

Brain Region	Atlas Coordinates			T-value	Z-score	Effect size \ddagger	P-value
	X	Y	Z				
pAD (n=74) versus Normal Controls (n=82)							
Posterior Cingulate	-8	-51	32	9.3	7.6	1.43	4.40 $\times 10^{-7}$
Precuneus	Left	-8	-54	25	9.0	1.48	4.4 $\times 10^{-16}$ *
	Right	8	-51	25	9.9	1.57	4.4 $\times 10^{-16}$ *
Parietal	Left	-52	-48	43	6.8	0.87	2.5 $\times 10^{-11}$
	Right	50	-52	39	9.3	1.33	4.4 $\times 10^{-16}$ *
Temporal	Left	-64	-34	-14	7.6	0.67	1.8 $\times 10^{-14}$
	Right	66	-34	-14	7.8	1.14	5.6 $\times 10^{-14}$
Frontal	Left	-26	27	31	4.3	0.54	1.4 $\times 10^{-5}$ *
	Right	44	22	50	4.5	0.70	4.0 $\times 10^{-6}$ *
Medial Temporal	Left	-36	-35	-8	5.3	0.61	1.1 $\times 10^{-7}$
	Right	34	-35	-8	4.3	0.62	1.0 $\times 10^{-5}$
Occipital	Left	-40	-72	37	7.2	1.21	2.1 $\times 10^{-12}$
	Right	36	-62	33	6.1	1.05	2.2 $\times 10^{-9}$ *
aMCI (n=142) versus Normal Controls (n=82)							
Posterior Cingulate	-2	-32	32	4.1	4.0	0.52	2.8 $\times 10^{-5}$ *
Precuneus	Left	-6	-51	36	3.3	0.48	5.9 $\times 10^{-4}$ *
	Right	6	-49	28	5.3	0.71	1.5 $\times 10^{-7}$ *
Parietal	Left	-42	-60	36	3.9	0.44	4.7 $\times 10^{-5}$ *
	Right	48	-50	39	4.0	0.60	4.2 $\times 10^{-5}$ *
Temporal	Left	-42	-56	14	3.3	0.51	4.9 $\times 10^{-4}$ *
	Left	-22	29	32	4.4	0.62	6.2 $\times 10^{-6}$ *
Frontal	Right	48	29	36	3.3	0.45	5.5 $\times 10^{-4}$ *
	Left	-40	-62	25	3.6	0.56	1.8 $\times 10^{-4}$ *

The reported significance levels are uncorrected for multiple comparisons ($p < 0.001$);

* each remained significant ($p < 0.05$) after false discovery rate (FDR) correction

[‡] Bias Corrected (Hedge's g) Effect size

[†] Atlas coordinates for the maximal CMRgl reductions were obtained from Talairach and Tournoux (1988). X is the distance to the right (+) or left (-) of the midline, Y is the distance anterior (+) or posterior (-) to the anterior commissure, and Z is the distance superior (+) or inferior (-) to a horizontal plane through the anterior and posterior commissures.

TABLE 3

Location and magnitude of the most significant correlations between disease category (CDR score 0, 0.5 and 1.0) and lower regional-to-whole brain CMRgl (N = 298)

Brain Region	Atlas Coordinates			Correlation Coefficient	Z-score	P-value
	X	Y	Z			
Posterior Cingulate	-8	-51	32	-0.47	7.6	1.1×10^{-16}
Precuneus	Left	-8	-53	24	-0.46	1.1×10^{-16}
	Right	8	-51	25	-0.49	4.4×10^{-16}
Parietal	Left	-53	-47	36	-0.42	2.5×10^{-14}
	Right	50	-51	39	-0.47	4.4×10^{-16}
Temporal	Left	-63	-34	-12	-0.41	4.8×10^{-14}
	Right	67	-32	-12	-0.41	5.9×10^{-14}
Frontal	Left	-26	27	33	-0.24	1.2×10^{-5}
	Right	45	27	35	-0.26	1.9×10^{-6}
Medial Temporal	Left	-59	-49	-8	-0.36	6.3×10^{-11}
	Right	67	-32	-12	-0.41	5.9×10^{-14}
Occipital	Left	-38	-73	41	-0.37	3.2×10^{-11}
	Right	36	-62	33	-0.26	3.9×10^{-6}

The reported significance levels are uncorrected for multiple comparisons ($p < 0.001$).

[†]Atlas coordinates for the maximal CMRl reductions were obtained from Talairach and Tournoux (1988). X is the distance to the right (+) or left (-) of the midline, Y is the distance anterior (+) or posterior (-) to the anterior commissure, and Z is the distance superior (+) or inferior (-) to a horizontal plane through the anterior and posterior commissures.

TABLE 4

Location and magnitude of the most significant correlations between MMSE and lower regional-to-whole brain CMRgl (N = 298)

Brain Region	Atlas Coordinates			Correlation Coefficient	Z-score	P-value	
	X	Y	Z				
Precuneus	Left	-6	-49	36	0.36	6.3	1.4×10^{-10}
	Right	12	-49	28	0.37	6.6	1.2×10^{-11}
Parietal	Left	-51	-52	40	0.26	4.6	3.1×10^{-10}
	Right	50	-52	43	0.36	6.5	4.5×10^{-11}
Temporal	Left	-63	-34	-12	0.43	7.2	5.9×10^{-15}
	Right	65	-32	-12	0.32	5.7	5.7×10^{-9}
Frontal	Left	-26	49	5	0.23	3.9	3.9×10^{-5}
	Right	38	24	43	0.22	3.8	6.8×10^{-5}
Occipital	Left	-40	-72	33	0.31	5.5	2.1×10^{-8}
	Right	34	-59	32	0.22	3.9	4.9×10^{-5}

The reported significance levels are uncorrected for multiple comparisons ($p < 0.001$).

[†] Atlas coordinates for the maximal CMRgl reductions were obtained from Talairach and Tournoux (1988). X is the distance to the right (+) or left (-) of the midline, Y is the distance anterior (+) or posterior (-) to the anterior commissure, and Z is the distance superior (+) or inferior (-) to a horizontal plane through the anterior and posterior commissures.

TABLE 5

Location and magnitude of the most significant correlations between MMSE and lower regional-to-whole brain CMRgl in participants with probable Alzheimer's disease (n = 74)

Brain Region	Atlas Coordinates			Correlation Coefficient	Z-score	P-value
	X	Y	Z			
Temporal	Left -63	-26	-16	0.39	3.6	1.9×10^{-4}
Frontal	Left -16	48	34	0.44	4.1	2.1×10^{-5}
Fusiform	Left -32	-24	-22	0.40	3.7	1.1×10^{-4}
Striatum	Left -18	16	-1	0.35	3.1	9.53×10^{-4}

The reported significance levels are uncorrected for multiple comparisons ($p < 0.001$).

[†] Atlas coordinates for the maximal CMRgl reductions were obtained from Talairach and Tournoux (1988). X is the distance to the right (+) or left (-) of the midline, Y is the distance anterior (+) or posterior (-) to the anterior commissure, and Z is the distance superior (+) or inferior (-) to a horizontal plane through the anterior and posterior commissures.